Journal of Minerals & Materials Characterization & Engineering, Vol. 10, No.10, pp.973-987, 2011
jmmce.org

Studies on the Effect of Ba^{2+} on Growth, structural, Morphology, Optical, and Mechanical Properties of L-Valinium Picrate

K. Russel Raj and P. Murugakoothan*

PG & Research Department of Physics, Pachaiyappa's College, Chennai – 600 030, India

*Corresponding author: Murugakoothan03@yahoo.co.in

ABSTRACT

Single crystals of undoped (pure) and barium nitrate (Ba $(NO_3)_2$)-doped L-Valinium Picrate (LVP) were grown from aqueous solution by slow evaporation technique. Morphological changes have been observed when Ba $(NO_3)_2$ is doped into LVP crystals. The dopant concentration in the crystals was measured by ICP technique. Slight changes in the unit cell parameter of LVP after doping with Ba $(NO_3)_2$ have been detected. The powder X-ray diffraction of the grown crystals has been recorded and the various planes of reflection identified shows shift in the peak positions. FTIR and UV spectra reveal the functional group identification and optical property of the grown crystals. The relative second harmonic generation (SHG) efficiency measurements revealed that both 5 and 10 mol % of Ba $(NO_3)_2$ in LVP enhanced the SHG efficiency by 92.85 and 160.59 times that of KDP respectively. However, at higher concentration, SHG efficiency is not increased but rather decreased from it undoped condition. Microhardness studies show that hardness number (Hv) increased with increase in load for all the grown crystals of this work.

Key Words: *A1. Doping; A1. Solutions; A2. Growth from solutions; B2. Nonlinear optic materials.*

1. INTRODUCTION

It is well know that the deliberate selection of reaction reagents is crucial to produce more efficient NLO materials of good quality. Amino acids are widely utilized because they not only contain chairal carbon atoms directing the crystallization in non centrosymmetric space group, but also possess zwitterionic nature favoring crystal hardness [1, 2]. Growth of nonlinear optical

(NLO) single crystals with good quality initiates the development of many novel devices in the field of optoelectronic and optical communications such as optical modulator, optical data storage and optical switches [3, 4]. Due to the wide area of applications, researchers are attracted towards this field. Although a large number of NLO materials have been identified and reported, each material has some limitations. Hence, the search for an ideal NLO material is still continuing. Since the material possessing amino acid groups attached to the phenyl rings have great potential with respect to other materials due to large contribution of the electron-phonon part to the corresponding hyperpolarizabilities [5]. The influence of impurities on the growth behavior has attracted intensive studies; impurities have various effects both in habit modification and crystal quality [6-8]. In the present investigation the SHG property of the LVP with addition of different mol percentage of Ba $(NO_3)_2$ were determined by Kurtz powder method. We observed high enhancement in SHG efficiency for 5 and 10 mol % of Ba $(NO_3)_2$. The crystalline perfection has a strong influence on the efficiency of the physical properties [9]. The influence of impurities on the growth behavior has attracted intensive studies both in habit modification and crystal quality [10-12]. In the present communication, in addition to the growth of pure and Ba^{2+}-doped LVP, we report the effect of the dopant-Ba^{2+} in LVP on growth, structural, optical, and mechanical properties by powder XRD, FT-IR, UV-Vis-NIR, Kurtz powder, and Vickers hardness measurements.

2. EXPERIMENTAL PROCEDURE

2.1. Growth Procedure

The pure L-Valinium Picrate has been synthesized from an aqueous solution containing L-Valine (Loba Chemie) and Picric acid (Qualigens) in 1:1 stoichiometric ratio by slow evaporation technique at room temperature. The synthesized L-Valinium Picrate is recrystalaized several times. The LVP crystals are grown from the recrystalaized saturated solution. The seed crystals are obtained in a period of 3 days using slow evaporation method. Bulk crystals are grown from the saturated solution of LVP, in a crystallizer, using submerged seed solution evaporation method. The Ba^{2+}: LVP crystals are grown from the saturated solution of LVP mixed with 5, 10, 15 mol. % of Barium nitrate salt. The solution is stirred continuously for 3 hours for homogenization. The resulting solution is filtered twice and allowed to evaporate. The crystal growth rate and quality are good when the pH is maintained at 2.34. Large numbers of small transparent seed crystals with perfect shape and free from macroscopic visible defects are grown in 3 days. Among these, well-shaped good quality crystals are screened using optical microscope and are selected as seed crystals. Bulk crystals are grown, using these seeds, from the saturated solution of Ba^{2+}: LVP in a crystallizer using submerged seed solution slow evaporation method. The grown crystals are shown in Figure 1. Growth rate and morphology of Ba^{2+}: LVP crystals are good compared with that of pure LVP.

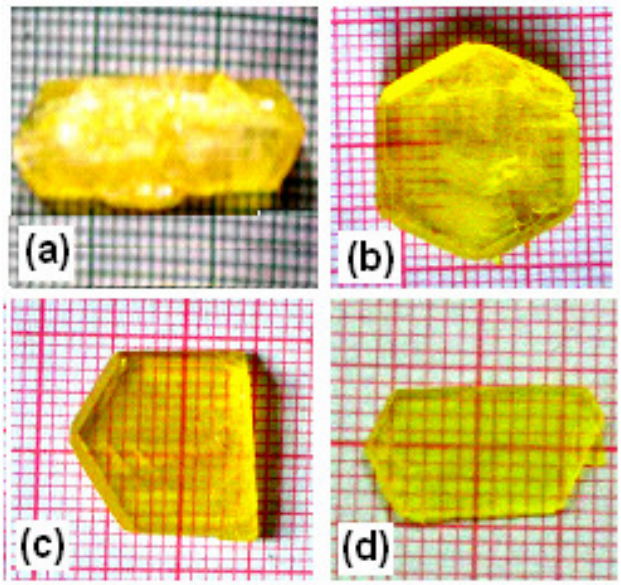

Figure 1. As grown crystal, (a) Pure LVP, (b) Ba^{2+}: LVP (0.05 mol), (c) Ba^{2+}: LVP (0.10 mol), (d) Ba^{2+}: LVP (0.15 mol)

2.2. Solubility of Ba^{2+}: LVP

The solubility studies for pure and Ba^{2+}-doped LVP (Ba^{2+}: LVP) with barium nitrate concentrations 5, 10, 15 mol % in deionized water have been performed in the temperature range between 30 ^{0}C and 50 ^{0}C in steps of 5 ^{0}C. The temperature of the solution is maintained at a chosen constant temperature and solution is continuously stirred using a motorized magnetic stirrer to ensure homogeneous temperature and concentration throughout the volume of the solution, and then the solubility is gravimetrically determined. The same process is repeated for different temperatures and the solubility curve obtained is shown in Figure 2. It is found that the solubility of Ba^{2+}: LVP increases with increase in temperature. Since the solubility curve is neither flat nor steep, it is possible to adopt both slow evaporation and slow cooling method for the growth of Ba^{2+}: LVP.

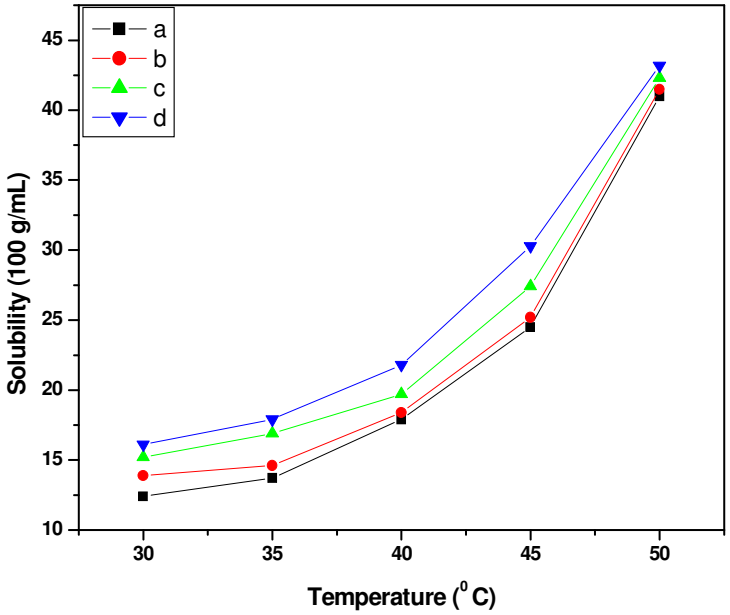

Figure 2. Solubility curve of (a) Pure LVP, (b) Ba^{2+}: LVP (0.05 mol), (c) Ba^{2+}: LVP (0.10 mol), (d) Ba^{2+}: LVP (0.15 mol)

3. MATERIAL CHARACTERIZATION

In order to estimate the crystal structure and morphology of pure and barium doped LVP crystals, single crystal X – ray diffraction studies have been carried out using Enraf Nonius CAD4 diffractometer with Mo Kα (λ = 0.7170 Å). Powder X-ray diffraction studies have been carried out for pure LVP and Ba^{2+}: LVP single crystals using a Rich Seifert X-ray Diffractometer with CuKα (λ = 1.5405Å) radiation over the range 10 ° – 70 ° at a scan rate of 0.02 °/ second for indexing the lattice planes. The presence of metals in the crystal lattice of grown crystals is determined by ICP technique (Inductively coupled plasma emission). The FTIR spectra of pure LVP, Ba^{2+}: LVP crystals have been recorded on BRUKER IFS FT-IR spectrometer using KBr pellet method in the range 400 – 4000 cm^{-1} to reveal the functional groups. The optical absorption spectra of pure LVP and Ba^{2+}: LVP single crystals are recorded in the region 200 – 2000 nm using Varian Carry SE model spectrometer to study their transmission behavior to electromagnetic radiation. The second harmonic generation (SHG) test on the Ba^{2+}: LVP crystals have been performed by the Kurtz and Perry powder SHG method [13]. The hardness of the Ba^{2+}: LVP crystal is determined using the Reichert MD 4000E ultra micro hardness tester fitted with a Vickers diamond pyramidal indenter attached to a Reichert Polyvar 2 MET microscope.

4. RESULTS AND DISCUSSION

4.1 X- ray Diffraction Analysis

The single crystal samples of LVP and Ba^{2+}: LVP having dimensions of 9 x 4 x 1 mm^3 have been subjected to X – ray analysis. The experimental unit cell parameters obtained coincides with that of Anita et al. [14]. The crystallinity of pure and Ba^{2+} doped LVP single crystals are confirmed by powder X – ray diffraction analysis. The diffraction peaks are indexed from crystal structure parameters obtained in the present study and are shown in Figure 3. The variations in lattice parameters, intensity of peaks and increase in cell volume for Ba^{2+} doped LVP clearly indicate that barium could be incorporated in to the pure LVP crystal lattice. Powder XRD analysis confirm the fact that the structure of LVP crystal slightly changes, as observed from the changes in peak intensities due to doping, which may be attributed to strains in the lattice [15].

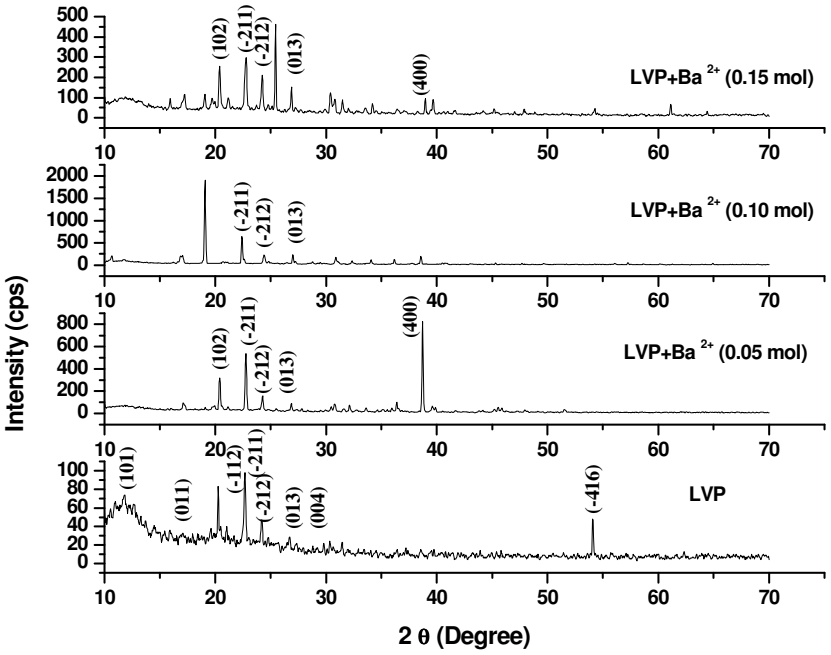

Figure 3. Powder XRD comparison of (a) Pure LVP, (b) Ba^{2+}: LVP (0.05 mol), (c) Ba^{2+}: LVP (0.10 mol), (d) Ba^{2+}: LVP (0.15 mol)

4.2 Inductively Coupled Plasma Emission Analysis

The presence of barium in the crystal lattice is determined by inductively coupled plasma emission analysis (ICP). Experimental results are depicted in Table 1.

Table 1. Percentage of Ba^{2+} in LVP doped with 0.05, 0.10, 0.15 mol of Ba^{2+} from ICP analysis.

Sample ID	Weight (g)	Analyte (Barium Nitrate)	Mean	Wt % of Barium
LVP+0.05 mol of Ba^{2+}	0.04193	233.527	1.085 mg/L	0.064691
LVP+0.10 mol of Ba^{2+}	0.04191	233.523	0.985 mg/L	0.058756
LVP+0.15 mol of Ba^{2+}	0.4058	233.527	2.062 mg/L	0.127033

4.3 Morphology Analysis

The studies on surface morphology and growth mechanisms of crystals are useful to know about the mechanism of crystal growth and thereby to eliminate the defects, enhance the growth rate and improve the quality [16]. The morphology of growing crystal is broadly governed by two factors, the internal structure of the crystal and external parameters such as supersaturation, temperature level, orientation of the seed, the presence of solvent and impurities. The important parameters controlling the growth rate are the energy required to create a step at the crystal surface and free-energy barrier for an adsorbed impurity ions to be incorporated in to the crystal. If the surface relaxations are large enough then small nuclei will grow into platelets, although large nuclei still grow into large three dimensional crystals [17]. Well developed morphological faces of Ba^{2+}: LVP may be due to the surface relaxation effect caused by the inclusion of Ba^{2+} in to LVP. In comparison with the irregular morphology exhibited by the pure LVP (Figure 2a), the presence of Ba^{2+} in the solution controls the growth rate in all directions and leads to produce prismatic shape and good size for the Ba^{2+}: LVP (Figure 2c). The positions of the Ba^{2+}: LVP crystal for (100), (001) and (-111) planes are observed, and hence, the crystallographic axes a, b and c have been determined. The main reason for the change in crystal morphology is the modification of the growth rates in crystallographic axes due to surface relaxation by the dopant barium. In Ba^{2+}: LVP, the growth rate is anisotropic; it is high along the b axis relative to the growth along a and c axes. This increase of the growth rate of the (100) plane of Ba^{2+}: LVP crystal is caused by a decrease of the Gibbs energy Δ_G $^{(010)}$ of the deposition process [18]. The morphology of Ba^{2+}: LVP, shown in Figure 4, establishes that there are six well developed faces, out of which the (100), (001) and (-111) planes are more prominent. The lower growth rate of other faces shows that the growth is energetically more difficult on these faces and the crystallization is probably limited by the process of staking of growth units on these crystal planes. In view of the available growth environment containing barium, it seems that the prismatic shapes are produced by the occurrence of two dimension nucleation, when the supersaturation at some planes on the growing crystal is higher than that at the rest of the planes. Due to this local increased supersaturation, these planes act as two dimensional nucleation centers. Morphological changes are observed in barium doped LVP crystals and compared with

pure LVP, these changes revealed that the bivalent impurities such as Ba^{2+} form chain like structure and disturb the crystal lattice more strongly than trivalent ions [15].

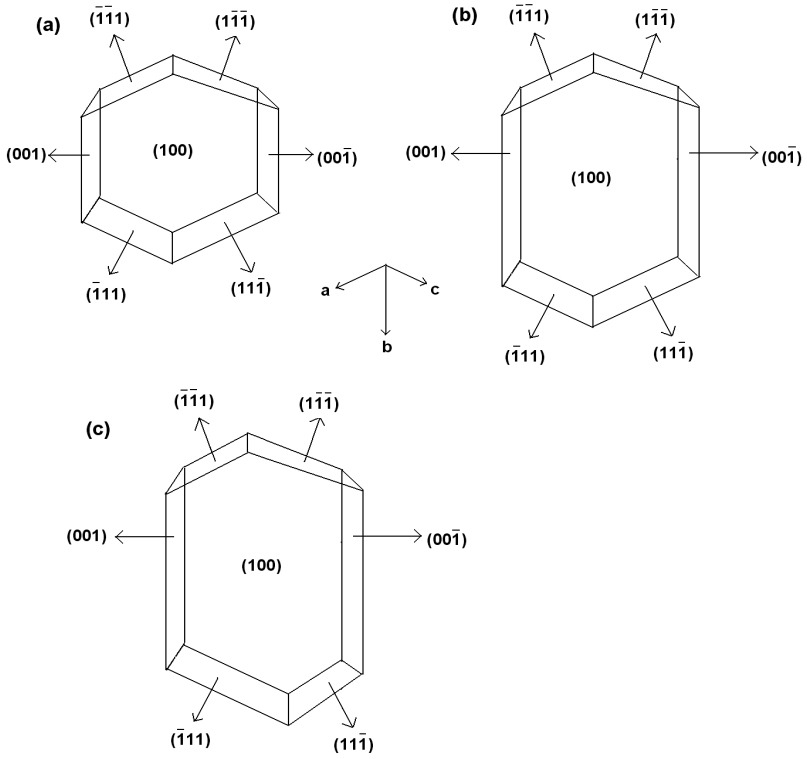

Figure 4. Morphology curve of (a) Ba^{2+}: LVP (0.05 mol), (b) Ba^{2+}: LVP (0.10 mol), (c) Ba^{2+}: LVP (0.15 mol)

4.4 FT-IR Studies

The FT-IR spectra of pure LVP, Ba^{2+}: LVP crystals are recorded on BRUKER IFS FT-IR spectrometer using KBr pellet method in the range 400 – 4000 cm^{-1} and are shown in Figure 5 for functional groups. All the absorption frequencies and their assignments are listed in Table 2. The structure of LVP includes a weak intramolecular and a strong intermolecular hydrogen bonding between the picrate anion and L-Valinium residue, which is characterized by O–H…O hydrogen bonding. The amino N atom of the L-Valinium cation forms N-H…O hydrogen bonds with the O atoms of the picrate anion. In addition, an intermolecular N-H…O hydrogen bond with the O atoms of carboxyl group also exists [20, 21]. The absorption at 3670–3580 cm^{-1} is due to the vibration of hydroxyl groups that are hydrogen bonded to aromatic ring π – electrons [22]. In barium doped LVP, the frequency of this band is shifted to lower wave number region 3420 cm^{-1} due to the addition of barium in to the intermolecular hydrogen bonds formed by picric acid

with L- Valinium. The broad envelope between 2400 cm^{-1} and 3700 cm^{-1} includes vibrations due to N-H stretching (3253 cm^{-1}), symmetric stretching of NH_3^+ at 2968 cm^{-1} and O-H stretching by hydrogen bonding. The C=O bond, usually strong, can be found in the 1710–1750 cm^{-1} region [23]. In pure LVP, the carboxylic acids are associated through H – bonds (which lower the frequency of the carbonyl) and absorb around 1715 cm^{-1} region. In Ba^{2+}: LVP, this absorption is around 1716 cm^{-1}. The peak at 1329 cm^{-1} is due to C–H deformation. The peak at 1271 cm^{-1} is due to CH_3/CH_2 deformation. The amide I vibration, absorbing near 1647 cm^{-1} arises mainly from the C=O stretching vibration, the C-C-N deformation and the N-H in plane bending [24]. The skeletal vibrations of aromatic rings observed at 1613 cm^{-1}, 1590 cm^{-1} are due to NH_3^+ asymmetrical deformation and NH_3^+ asymmetrical bending respectively. The peak at 1118 cm^{-1} and 1085 cm^{-1} are due to C–N stretching respectively. The peaks at 914 cm^{-1} and 542 cm^{-1} are due to C–C stretching and C–C deformation respectively. The band at 789 cm^{-1} confirms the C–C skeletal stretching. From the spectroscopic investigations, the presence of all the fundamental functional groups of the grown samples is confirmed qualitatively. Slight changes in the peak positions and intensities in FT-IR spectrum of Ba^{2+}: LVP in comparison with pure LVP is may be due to strain introduced in to the lattice by the metal dopants [16].

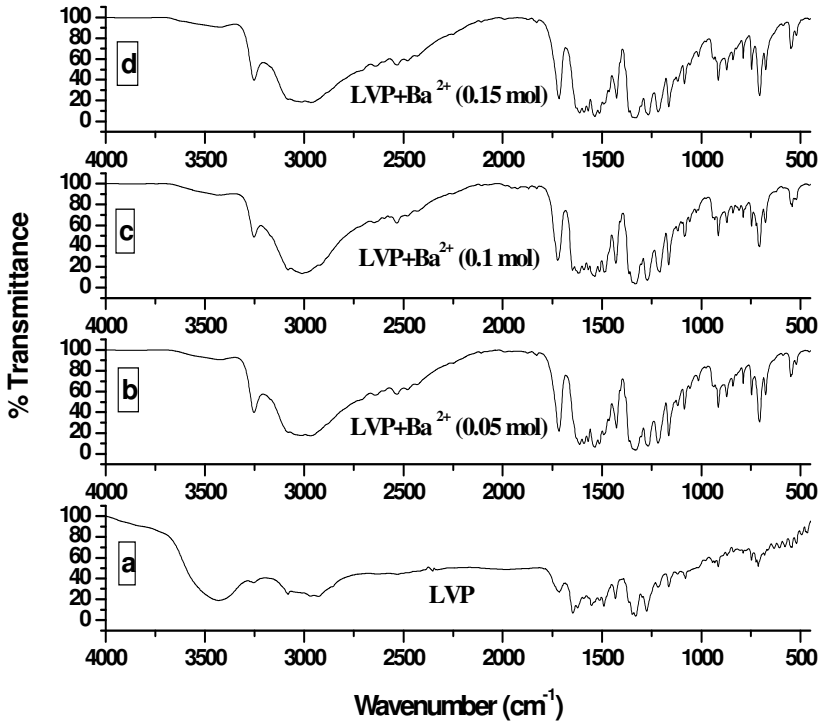

Figure 5. FT-IR spectrum of (a) Pure LVP, (b) Ba^{2+}: LVP (0.05 mol), (c) Ba^{2+}: LVP (0.10 mol), (d) Ba^{2+}: LVP (0.15 mol)

Table 2. FTIR spectral data of pure LVP and Ba^{2+}: LVP.

Wave number (cm^{-1})					Tentative assignment
	LVP	Ba^{2+}: LVP (0.05)	Ba^{2+}: LVP (0.10)	Ba^{2+}: LVP (0.15)	Ba^{2+}: LVP	LVP
Present work		Present work			Reported [24]	
3434	-	-	3418	-	O-H stretching	
-	3252	3252	3252	3252 m	N-H stretching	
2927	3013	3010	3014	3013 b	NH_3^+ symmetrical stretching	
2352	2532	2534	2641	-	N-H stretching	
1715	1716	-	1716	1718 s	C=O stretching	
1647	-	1648	1648	-	C=C stretching	
-	1611	1619	1612	1614 s	NH_3^+ asymmetrical deformation	
-	1590	1591	1590	-	NH_3^+ asymmetrical bending	
-	1570	1569	1570	1570 m	N-H deformation	
1552	1535	1537	1536	1537 s	NH_3^+ symmetrical stretching	
-	1513	-	1513	-	C-C strtching, phenyl ring skeletal	
1490	1491	1488	1491	1487 m	CH_3 asymmetrical deformation	
1432	1427	1430	1426	1429 s	C-O stretching + O-H in plane deformation	
1330	1330	1364	1363	1337 s	C-H deformation	
1275	1267	1272	1266	1269 s	CH_3 deformation / CH_2 deformation	
1217	1218	1209	1217	1215 s	C-O stretching +O-H stretching	
1164	1164	1164	1163	1161 s	C-O stretching	
-	1118	1118	1118	1119 w	C-N stretching	
1079	1085	1084	1085	1082 m	C-N stretching	
-	1014	1025	1014	1016 w	C-O stretching	
-	-	932	936	937 w	C-H out of plane deformation	
914	914	914	914	912 m	C-C stretching	
-	872	871	871	870 m	C-C-N symmetrical stretching	
-	840	840	839	839 w	C-H out of plane deformation	
789	789	789	789	787 m	C-C skeletal stretching	
747	746	746	746	-	NO_2 wagging	
713	706	706	705	706 s	N-H bending	
633	676	616	675	-	C-H out of plane deformation	
543	549	542	548	544 m	C-C deformation	
520	-	-	521	-	NO_2 scissoring	
493	-	-	-	-	C=O bending (out of plane)	

s - strong, m - medium, w - weak, b - broad

4.5 Linear and Nonlinear Optical Studies

Nonlinear optical single crystals are mainly used in optical applications. The optical transmission range, transparency cut-off and absorbance band are the most important optical parameters for laser frequency conversion applications. To find the transmission range of Ba^{2+} doped LVP, the optical transmission spectrum is observed for the wavelength between 200 to 2000 nm. A crystal thickness 2 mm is used for this measurement. The transmission spectra of the grown crystals are shown in Figure 6. It is observed from the figure that all the grown crystals have good transmission in the entire visible region. The doped crystals have better transmission compared to pure crystal. The Ba^{2+} doped LVP is optically transparent in the entire UV region and lower cut-off wavelength 410 nm, is sufficient for SHG laser radiation of 1064 nm or other application in the blue region. The Tauc's graph between the product absorption coefficient and the incident photon energy $(\alpha h\nu)^2$ with the photon energy $h\nu$ at room temperature shows a linear behavior that can be considered as evidence of the direct transition. The optical band gap (E_g) of Ba^{2+}: LVP for 5, 10, 15 mol % crystals have been estimated by extrapolation of the linear portion near the onset of absorption edge to the energy axis [25] is shown in Figure 7. From the Figure (7), value of optical band gap energy (Eg) of Ba^{2+}: LVP for 5, 10, 15 mol % crystals are found to be 2.29, 5.17 and 5.43 eV respectively.

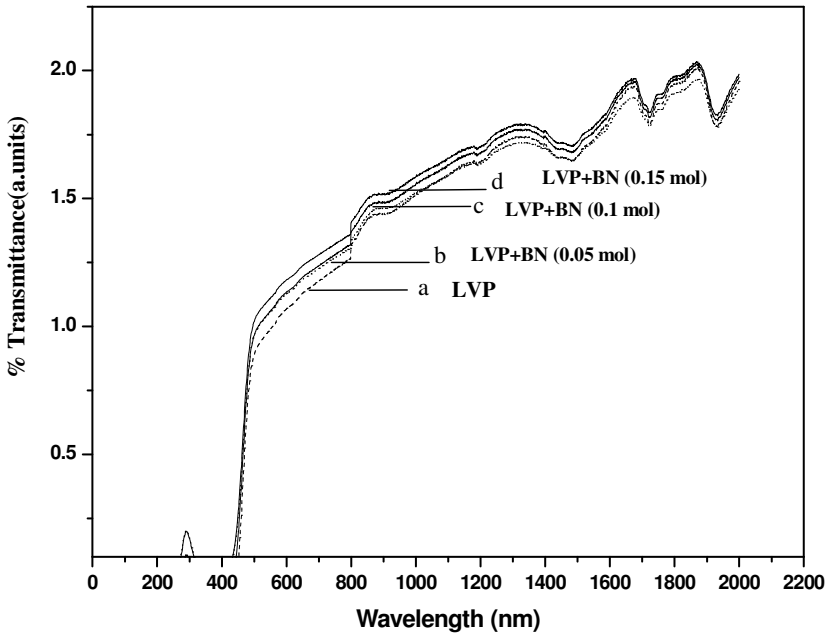

Figure 6 Optical transmittance curve of (a) Pure LVP, (b) Ba^{2+}: LVP (0.05 mol), (c) Ba^{2+}: LVP (0.10 mol), (d) Ba^{2+}: LVP (0.15 mol).

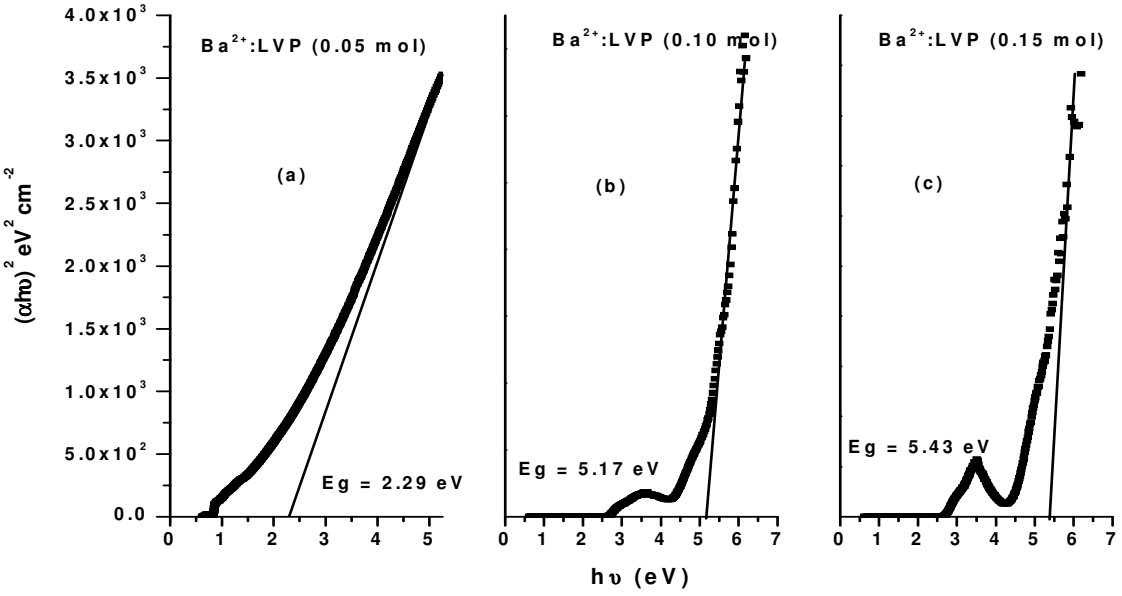

Figure 7 Energy band gap curve of (a) Ba^{2+}: LVP (0.05 mol), (b) Ba^{2+}: LVP (0.10 mol), (c) Ba^{2+}: LVP (0.15 mol).

4.6 Second Harmonic Generation Studies

Essentially second order NLO effect in organic molecule originates from a strong donor – acceptor intermolecular interaction in particular system, which lacks a centre of symmetry [26]. The pure LVP contains a valine cation and a picrate anion where the carboxyl group is protonated. Thus a π-π^* transition occurs in the carboxyl group, which gives rise to NLO properties in the system [27]. Also the donor and acceptor molecule of L-valine and picric acid complex are held together by the contact of van der Waals type. Hence, the effect of intermolecular hydrogen bonding between the phenolate ion of picric acid and the L-valine residue will enhance the hyperpolarizability β value, which is the required property for a system to exhibit a nonlinear optical process [28]. It is also recognized that the first order electronic hyperpolarizability value β is enhanced when there is a low lying ground-to-excited state transition with large change in the dipole moment [29, 30]. In our present work, the emission of green radiation of 532 nm from the fundamental radiation of wavelength 1064 nm confirmed the doubling of frequency the SHG efficiency is enhanced for 5 and 10 mol % of Ba^{2+}: LVP by 92.84 and 160.49 times that of KDP respectively, which shows that these dopants have catalytic effect on the NLO properties. Doping of Ba^{2+} enhances second-order effect due to the favorable alignment of the molecules within the crystal structure [26]. The SHG efficiency decreases slightly with doping of crystal by 15 mol % of Ba^{2+}, which may be due to the disturbance of

charge transfer (CT). The attainment of second-order effect requires favorable alignment of the molecules through inclusion complexation greatly enhanced the SHG, [31] and also due to the level of SHG response of a given material is inherently dependent upon its structural attributes. On the molecular scale, the extent of charge transfer across the NLO chromospheres determines the level of SHG output [32]. The relative second harmonic generation efficiency of the crystals is presented in Table 3.

Table 3. Relative second harmonic generation efficiency of pure LVP and Ba^{2+}: LVP

System	Input beam energy mJ/Pulse	Output (Volt)	KDP (mV)	Relative Second Harmonic efficiency
LVP				60.00
LVP+0.05 mol of Ba^{2+}	4.20	1.3 V	14	92.84
LVP+0.10 mol of Ba^{2+}	4.99	0.085 V	0.529	160.49
LVP+0.15 mol of Ba^{2+}	4.20	0.690 V	14	49.28

4.7 Micro Hardness Studies

The hardness of the crystal determines the applicability of the crystal in the device fabrication. Measurement of hardness is a useful non destructive testing method used to determine the bond strength. The micro hardness value correlates with other mechanical properties such as elastic constant and yield strength. Indentations are made on the (100) face of the crystal and the micro hardness measurements have been made for the applied loads varying from 1 to 50 g for the dwell time of 3 s. The hardness of the crystal can be calculated using the relation $H_v = 1.8544\ P/d^2$ where H_v is the Vickers hardness number, P is the indenter load in gram and d is the diagonal length of the impression in millimeter. The results obtained in micro hardness values are shown in Figure 8. It is evident from the plot that the micro hardness value of the crystal increases with increasing load. The increase in the micro hardness values of Ba^{2+}: LVP with increasing load is in agreement with the reverse indentation size effect (RISE).

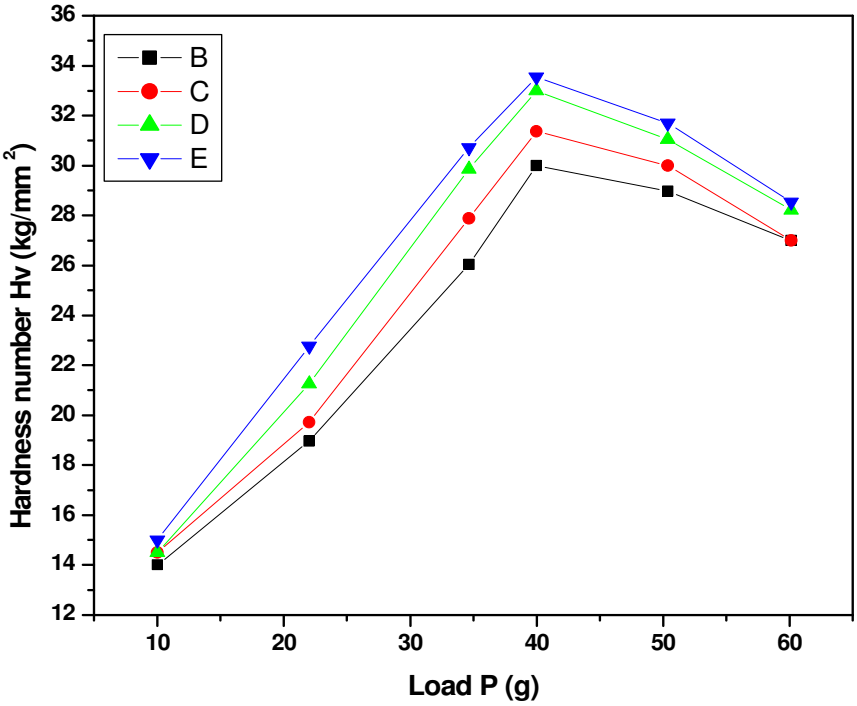

Figure 8 Microhardness curve of (a) Pure LVP, (b) Ba^{2+}: LVP (0.05 mol), (c) Ba^{2+}: LVP (0.10 mol), (d) Ba^{2+}: LVP (0.15 mol)

5. CONCLUSION

Optical quality crystals of pure and Ba^{2+}: LVP have been grown from aqueous solution in 15-20 days by submerged seed solution slow evaporation method. The solubility curve for Ba^{2+}: LVP in deionized water at various temperatures are determined. From the powder XRD pattern, various planes of reflections are identified for pure LVP and Ba^{2+}: LVP. The grown crystals are characterized by using single crystal X-ray diffraction which confirms the Ba^{2+}: LVP grows predominantly along b axis. The inductively coupled plasma emission result suggests that the amount of metallic dopant incorporated in to the crystal lattice is far below its original concentration in the solution. Morphological studies ascertained that the incorporation of Ba^{2+} in LVP has a great influence on crystal habit and rate of growth. The irregular morphology of pure LVP has been very much improved by the incorporation of Ba^{2+} into the lattice of LVP crystal. The presence of Ba^{2+} in LVP crystal lattice is qualitatively confirmed by FTIR analysis. The incorporation of Ba^{2+} has improved the optical transparency of the LVP crystal. The NLO

activity in the Ba^{2+}: LVP is confirmed by employing Nd: YAG laser as source. Micro hardness test on the Ba^{2+}: LVP crystal confirms the hardness behavior of the material.

REFERENCE

[1] Prasad, P. N., Williams, D. J., 1991, *Introduction to Nonlinear Optical Effects in Organic Molecules and Polymer*, Wiley, New York.

[2] Jiang, M. H., Fang, Q., 1999, *Adv. Mater.,*Vol, 11, pp. 1147

[3] Agarwal, M. D., Choi, J., Wang, W. S., Bhat, K., Lal, R. B., Shields, A. D., Penn, B. G., Frazier, D. V.,1999, *J. Cryst. Growth,* Vol. 179, pp. 2004.

[4] Jiang, M., Xu, D., Tan, Z., 1983, *Acta. Chem. Syn*., Vol.41, pp570.

[5] Ding, Y. J., Mu, X., Gu, X.,2000, *J. Nonlinear Opt. Phys. Mater*, Vol. 9 pp. 21.

[6] Kityk, I. V., MakowskaJanusik, M., Gondek, E., Krzeminska, L., Daniel, A., Plucinski, K. J., Benet, S., and Sahraoui, B., 2004, *J. Phys: Cond. Matter*, Vol.16 pp. 231.

[7] Bhavannarayana, G., Budakoti,G. C., Maurya, K. K., Kumar, B., 2005, *J. Cryst. Growth*, Vol. 282 pp. 394 - 401.

[8] Chen Jianzhong, Lin Sukun, Yang Fengtu, Wang Jiahe, and Lang Jianming, 1997, *J. Cryst. Growth,* Vol. 179, pp. 226.

[9] Kuznetsov, V. A., Oknrimenko, T. M., Miroslawa Rak, 1998, *J. Cryst. Growth,* Vol. 193, pp. 164.

[10] Guohui Li, Xue Liping, Genbosu, Xinxin Zhuang, Zhengdong Li, and Youping He., *J. Cryst. Growth,* 2005, Vol. 274, pp 555.

[11] Krishan Lal, and Bhagavannarayana, G., 1989, *J. Appl. Cryst*, Vol. 22, pp. 209-215.

[12] Bhagavannarayana, G., and Kushwaha, S. K., 2010, *J. Appl. Cryst,* Vol. 43. pp.154-162.

[13] Kurtz, S. K., Perry, T. T., 1968, *J. Appl. Phys,* Vol. 39. Pp. 3798-3813.

[14] Anitha, K., Sridhar, B., and Raja ram, R. K., 2004, Acta *Cryst*, Vol. E60. pp.1530.

[15] Podder, J., Ramalingom, S., Narayana Kalkura, S., 2001, *Cryst. Res. Techno,* Vol. 36.pp. 549- 556.

[16] Jiang, X. N., Xu, D., Yuan, D. R., Lu, M. K., Sun, D. L., 2002, *Cryst. Res. Technol*, Vol. 6. Pp. 564 – 569.

[17] Lee et al, W. T., 1999, *J. Phys; Condens. Matter*, Vol. 11. Pp. 7385-7410.

[18] Novotny, *J. Proceeding of SPIE*. Vol. 4710. *Int. Conf. Thermo sense*, April. 2002, XXIV. pp. 1-4. Orlando, FL, USA.

[19] Rak, M., Eremin, N. N., Eremina, T. A., Kuznetsov, V. A., Ohkrimenko, T. M., Furmanova, N. G., and Efremova, E. P., 2005, ***J***. *Cryst. Growth*, Vol. 273. pp. 577.

[20] Martin Britto Dhass., and Natarajan, S., 2008, *Cryst. Res. Technol*, Vol. 43.No. 8, 869 - 873

[21] Anitha, K., Sridhar, B., and Raja ram, R. K., 2004, *Acta Cryst,* Vol. E60. pp. o1530 – o1532.

[22] Socrates, G., 2001, *Infrared and Raman Characteristic Group Frequencies*, 3rd ed. New York.

[23] Daniel R Palleros, 2000, *Experimental Organic Chemistry*, University of California, and Santa Cruz. John Wikley & sons Inc. pp. 690-692.
[24] Socrates, G., 1980, *Infrared and Characteristic Group Frequencies*, John Wiley & sons: Singapore.
[25] Devis, E. A., Mott, N. F., *Philos. Mag*, Vol. 22. pp. 903.
[26] Lakshanana Perumal, C. K., Arulchakkaravathi, A., Prajesh, N., Santharaghavan,P., Ramasamy, P., 2002, *Mat. Lett*, Vol. 56. pp. 578.
[27] Pal, T., Kar, T., Boceli, G., Rigi, L., 2004, *Crystal Growth Des*, Vol. 4. pp. 743-747.
[28] Hall, S. R., Kolinsky, P. V., Jones, R., Allen, S., Gordon, P., Boshwell, B., Norman, P. A., Hursthouse, M., Karaulov, A., Baldwin, J., 1986, *J.Crystal. Growth*. 79. pp. 745.
[29] Thompson, W. H., Blanchard-Desce, M., Muller, A. J., Fort, A., Barzovkan, M., Hynes, J. T., 1999, *J. Phys. Chem*. Vol. A 103. pp. 3766.
[30] Shen, Y., 1984, *The Principles of Nonlinear Optics*, Wiley, New York.
[31] Hall, S. R., Kolinsky, P. V., Jones, R., Allen, S., Gorden, P., Boshwell, B., Bloor, D., Norman, A., J. Baldwin, 1986, *J. Crystal. Growth*. Vol. 79. pp. 745-751.
[32] Wang, Y., Eatus, D. F., 1985, *Chem. Phy. Lett*, Vol. 120. pp. 441-444.